

Experimental verification of the greenhouse effect

4. Communication: The near-Earth CO2 radiation

By Dr. Michael Schnell; January 2019

Abstract

Following public perception, CO₂ is an environmentally hazardous gas that has become an existential threat to humanity. By contrast, the actual CO₂ fraction of the global back radiation of 333 W/m² [1], [3], [4], [5] is likely to be largely unknown and will probably trigger astonished or incredulous head shaking when looking at Fig. 1. For a good reason, the IPCC avoids such an overview and prefers to discuss a fragile thermal equilibrium that is shifted by the smallest changes (CO₂ radiation force) [2]. Those who get involved in it end with the snowball effect (triggering an avalanche) and overlook the actually robust properties of the overall system. With a little logic and mathematics, the IPCC data can be used to determine the current CO₂ radiation of around 32 W/m² (10% of the global back radiation, Fig. 1, black curve). CO₂ thus occupies only fourth place in the atmospheric emitters (Fig. 21).

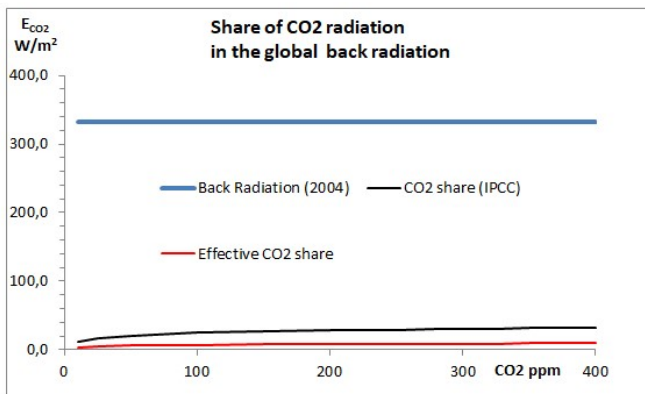


Fig. 1: The Near-Earth CO₂ radiation

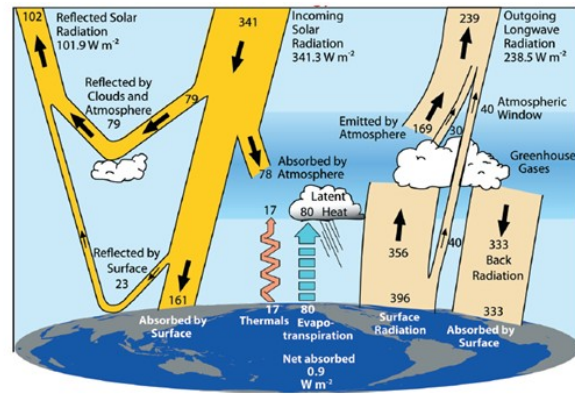


Fig. 2: Global energy balances in W/m² acc. to K.E. Trenberth [1]

Even this small value, is still too high. Water vapor, the invisible aerosols and above all the clouds are other actors of the atmospheric back radiation, which control and reduce each other (Fig. 21). It is already known that the CO₂ and water vapor radiation partially overlap, which reduces the CO₂ contribution in humid air [6], [7]. The interaction with the clouds/aerosols is another much more effective damper of the CO₂ effect. If the IPCC also considered these radiation competitors, the actual CO₂ greenhouse effect would be around 10 W/m² or 3% of global back radiation (Fig. 1, red curve).

With such a low amount of CO₂, one has to ask oneself whether the climate is really threatened by CO₂ and how atmospheric back radiation is to be understood. The principle of foreground and background radiation is a new approach to a better understanding of different atmospheric radiation sources. This thesis runs like a red thread through the publication series "Experimental Verification of the Greenhouse Effect". In the following, a CO₂ radiation formula, starting on J. Stefan's [8] findings and on the basis of the own laboratory experiments, is derived step by step. This results in a much lower CO₂ impact than assumed by the IPCC (Chap. 4, page 9).

1. Introduction

At the beginning of the 19th century, various groups of researchers were looking for a mathematical relationship between temperature and IR radiation of a body. Among other Dulong and Petit, who investigated the cooling of a hot thermometer (200 – 300 °C) in a cold vacuum vessel (Fig. 3) [9]. They developed a simple formula that accurately reflected the temporal cooling of the thermometer. However, the equation failed when substantially hotter bodies, such as those of the sun, should be calculated.

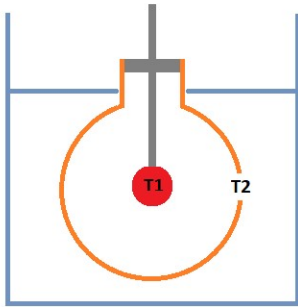


Fig. 3: Cooling of a heated thermometer T1 in a cooled copper vessel T2, after Dulong and Petit [9]

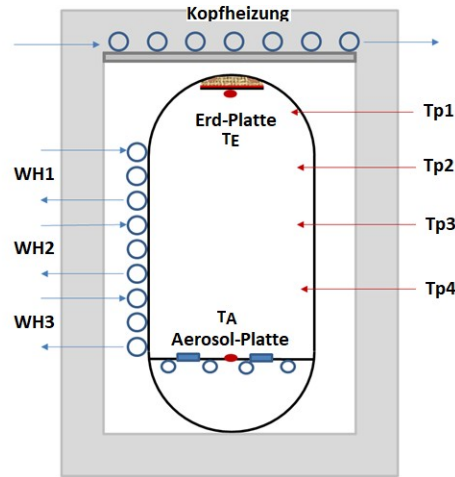


Fig. 4: Own apparatus with earth plate TE and aerosol plate TA

Josef Stefan reviewed the experiments of Dulong and Petit and other research groups and could purely empirical establish Eq. 1, whereby the heat transfer P of parallel surfaces, even at very high temperatures, could be calculated [8]. Stefan needed the so-called radiation exchange grade "E" for bright, reflective surfaces (emissivity $\epsilon \ll 1$). However, assuming black body radiation with $\epsilon = 1$, E becomes 1 and we have equation Eq. 2, the forerunner of the Stefan Boltzmann Law (Eq. 3), which was theoretically derived by Ludwig Boltzmann in 1884, a student of Stefan [10].

Eq. 1: $P = \sigma \cdot A \cdot E \cdot (T_1^4 - T_2^4)$ $E = \frac{1}{\frac{1}{\epsilon_1} + \frac{1}{\epsilon_2} - 1}$: A = area, ϵ = emissivity, E = degree of radiation exchange

Eq. 2: $P = \sigma \cdot A \cdot (T_1^4 - T_2^4)$ $P = (\sigma \cdot A \cdot T_1^4) - (\sigma \cdot A \cdot T_2^4)$: $\epsilon = 1, \sigma = 5,670367 \cdot 10^{-8}$, P = energy loss

Eq. 3: $M = \sigma \cdot A \cdot T^4$: Stefan-Boltzmann law, $\epsilon = 1$, M = radiance of a black body

With Eq. 2 Stefan provides the basis for the calculation of the greenhouse effect. The cooling of the thermometer (energy loss) depends on both the temperature T1 and T2, i.e. the difference between the radiation of the thermometer and the back radiation of the copper wall.

If you want to study the CO2 greenhouse effect according to Eq. 2 experimentally, you need two black surfaces with a sufficient temperature difference ($T_1 \gg T_2$). The own apparatus with a warm earth and a cold aerosol plate fulfils this requirement. The experimental set-up (Fig. 4) is very similar to the copper vessel of Dulong and Petit, except that the distance between the soil and aerosol plates has been increased. This creates not only an air space for the potential addition of IR-active gases, but also a third radiation surface, the side wall, which has a significant influence on the back radiation. To understand this, a very simple back radiation scheme is presented, which uses red (warm = T_V) and blue (cold = T_H) colors to indicate radiation sources of different temperatures.

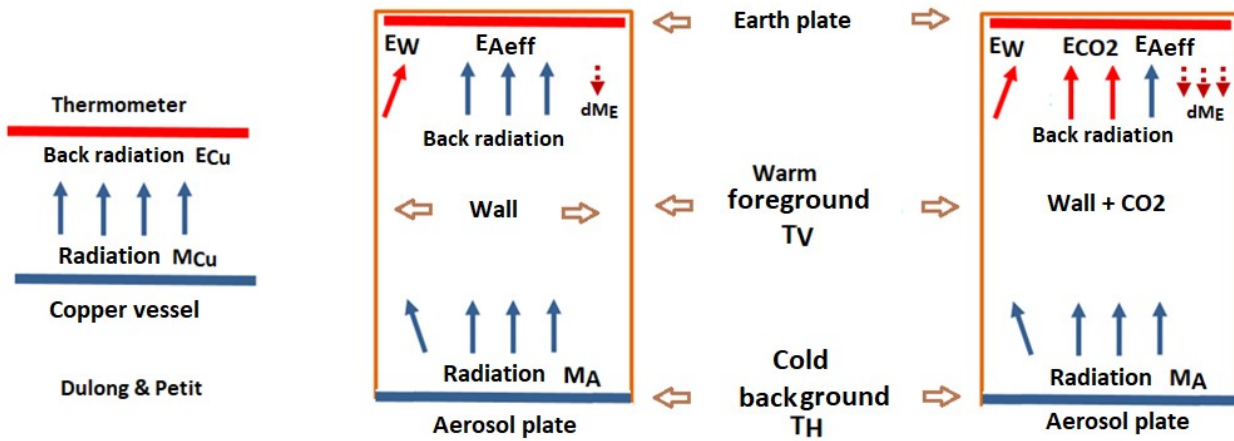


Fig. 5: Without side wall
Back radiation: $E_{Cu} = M_{Cu}$

Fig. 6: With side wall W
Back radiation: $E_W + E_{Aeff} > M_A$

Fig. 7: With side wall W + CO2
Back radiation: $E_W + E_{CO2} + E_{Aeff} \gg M_A$

Fig. 6 and 7 show the change in the back radiation, when a third radiation source, the sidewall and CO2, is added to the warm (red) and cold (blue) area in Fig. 5. From the point of view of the earth plate we now have two back radiators, which are defined as warm foreground (T_V , sidewall and CO2) and cold background (T_H , aerosol plate). Side wall and CO2 absorb some of the aerosol plate radiation (blue arrows) and emit their own, higher-energy radiation (red arrows), corresponding to their higher temperature T_V (Fig. 6, 7). The intervention of CO2 has four consequences:

A: Earth-Plate: CO2 increases the back radiation (2 red instead of 2 blue arrows). This results in a reduced release of energy (eq. 2) and creates a build-up of heat, which causes the earth plate to heat up until the energy loss and gain are equal again (Fig. 8). CO2 extracts the energy required for the radiation of its environment (see points C and D). CO2 is **no additional heat input** for the earth. Comparable with the Coriolis force is here a pseudo effect.

B: Aerosol-Plate: Not all photons of the aerosol plate reach the earth plate (1 blue arrow in Fig. 7). This fraction, which depends on the intensity of the foreground radiation, is the effective radiation of the aerosol plate E_{Aeff} [11]. In the background, however, the aerosol plate radiation M_A is constantly present as latent radiation.

C: Air-Temperature: The sidewall and CO2 lose energy, as their emission E_W/E_{CO2} (red arrows) is greater than their absorption (blue arrows), which would require the airspace to cool down. An already published demonstration experiment [12], [11] investigated the effects of CO2 (and other greenhouse gases) under adiabatic conditions (without wall heating). A significant warming of the earth plate was observed, while within the tube, at the measuring points Tp1 – Tp4, temperatures remained constant (Fig. 8 and 9). The constancy of the air temperature is explained by the radiance increase dM_E of the warmer earth plate (brown dotted arrows, Fig. 6 and 7), whereby heating and cooling effects are the same.

D: Energy balances: In the case of adiabatic experiment heating Q_E (input) and the energy transferred to the aerosol plate (output) must be the same (energy conservation law), independent from CO2. In order to establish this equality, the dry Earth surface can react with a temperature increase in a heat build-up by greenhouse gases (Fig. 8, Eq. 2). Oceans and wetlands can transfer the excess heat by evaporation of water to a layer of cloud even without IR radiation. These water surfaces would heat up little or no heat. In this case the CO2 greenhouse effect would cause a cooling of the atmosphere. If that could be proved, it would

turn the CO2 effect upside down and lead the water vapor feedback ad absurdum! An experimental investigation is still pending.

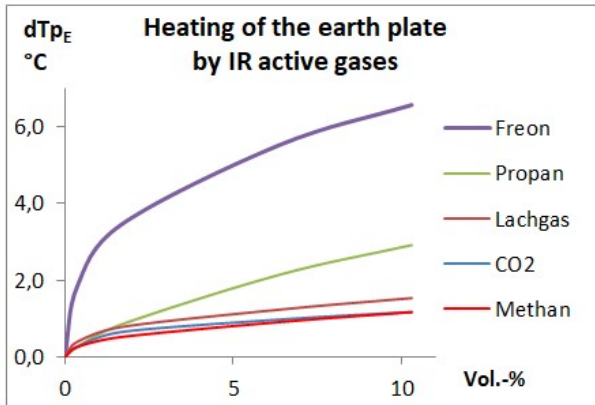


Fig. 8: Addition of greenhouse gases with constant heating Q_E without wall heaters (adiabatic radiation transport)

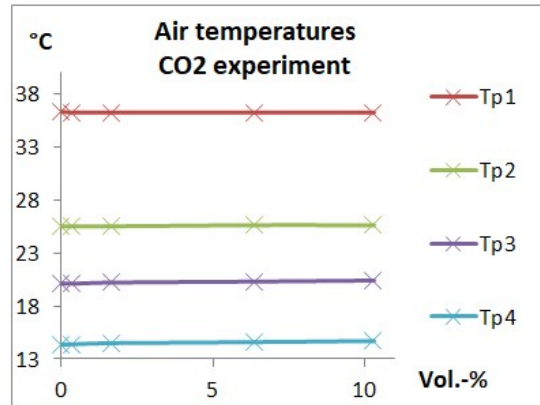


Fig. 9: Air temperatures at the measuring points Tp1 - Tp4 before and after adding CO2

The existence of an effective aerosol plate radiation E_{Aeff} according to point B) could be proved experimentally (Fig. 10 and 11). The basis is Eq. 4, which states that at constant temperature of the earth plate T_E (thermal equilibrium) energy loss (emission M_E) and energy supply (back radiation $E_A + E_W$ and heating Q_E) are equal. If the aerosol plate is gradually cooled in this experiment, the effective back radiation E_{Aeff} decreases. In order for T_E to remain constant, heating Q_E must be increased after each cooling step. If one plots Q_E over the temperature of the aerosol plate (as $T^4/10^8$), the trend is a straight line (red) with the increase $dQ_E/dT_{Aeff} = -4.18$ (Fig. 10).

$$\text{Eq. 4} \quad M_E = E_{Aeff} + E_W + Q_E \quad E_{Aeff} = M_E - E_W - Q_E \quad \epsilon_{Aeff} = M_A/E_{Aeff}$$

In Eq. 4 M_E and E_W are constants because their temperatures remain approximately constant. Heating Q_E and the effective radiation E_{Aeff} are variables and have, according to Eq. 4, the same increase but an opposite sign. The increase of this straight line E_{Aeff} is 4.18 and is smaller than the σ -constant (5.6703), which Stefan had determined empirically (Fig. 11, black line). The ratio of both numbers $4.18/5.67 = 0.74$ shows the attenuation of the aerosol plate radiation by the foreground side wall, or simply put, only 74% of the photons of the aerosol plate reach the earth plate [11]. The ratio of E_{Aeff}/M_A defines the effective emissivity of the aerosol plate radiation ϵ_{Aeff} .

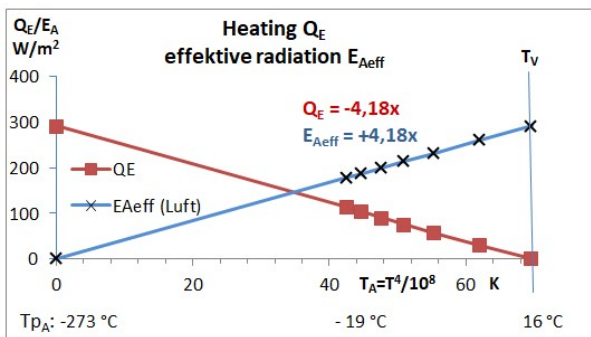


Fig. 10: Gradual cooling of the aerosol plate T_A Heating Q_E (red) and effective radiation E_{Aeff} (blue)

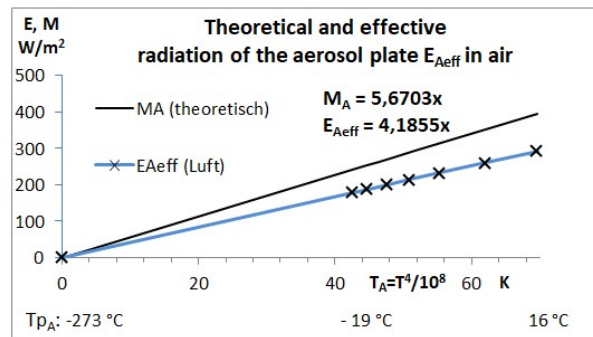


Fig. 11: Theoretical radiation (M_A) and effective radiation (E_{Aeff}) of the aerosol plate

If foreground and background are at the same temperature ($T_V = T_H$), $Q_E = 0$ (Fig. 10). Since one can construct a straight line with only two points, the increase can even be determined from a single heating value Q_E with the condition $T_V > T_H$ by Q_E/dT (one-point calibration). This technique is the basis for determining the CO2 emission levels (chapter 2).

The cooling experiment shows that the effect of a foreground radiation E_V can be determined by means of the heating Q_E . Prerequisite is a temperature difference between warm foreground and cold background, because at the same temperature ($T_V = T_H$) $Q_E = 0$. Or in other words, the greenhouse effect can only be experimentally proven against a cold background. At this request, all previous laboratory experiments from Al Gore to Wood have failed. Instead of the greenhouse effect, other physical effects (prevention of convection, heat conduction, or thermalization) have been observed [13], [14], [15].

2. CO2- Emissivity

Solid and liquid substances can be characterized by an average emissivity ϵ , which is influenced only by the nature of their surface, shiny or rough/dull. In the case of gases, this is fundamentally not possible since their radiation is also dependent on the number of their particles (mass). Concentration data (ppm or vol. %) can be used to characterize the number of particles, as long as temperature, pressure and volume are constant. But that's not the case with Earth's atmosphere. However, the CO2 number of molecules/m³ decreases sharply with increasing altitude. In order to be able to transfer the experiments to the CO2 radiation of the atmosphere, the number of CO2 molecules n (mol), which are between the 1.11 m distant earth and aerosol plates at a radiation cross-section of 1 m² (Eq. 5).

Eq. 5: $n = p \cdot V / (R \cdot T)$; $R = 8,314459 \text{ J}/(\text{mol} \cdot \text{K})$, $p = \text{pressure (Pa)}$, $V = 1,11 \cdot \text{Vol.-%} / 100 \text{ (m}^3\text{)}$, $T = \text{abs. temperature (K)}$

In order to determine the CO2 radiation, the CO2 concentration is gradually increased and the heating Q_E is reduced until the earth plate has exactly reached the starting temperature of +16.1 ° C. The modified heating Q_E then indicates the radiation amplification caused by CO2. However, since this amplification can only be measured with an already existing, as low as possible background radiation, the aerosol plate is cooled to a temperature as constant as possible of minus 15 ° C. Since the CO2 radiation also depends on the CO2 temperature, the entire airspace must have a uniform temperature (isothermal test conditions). This task is performed by the wall heaters WH1 to WH3.

The CO2 emissivities can be calculated from the effective emissivity of the aerosol plate radiation $\epsilon_{Aeff}(n)$, since foreground emitters change the effective radiation of the background, as described in Chap. 1 (Fig. 11). For this purpose, a first value (for $n = 0$, without CO2) according to Eq. 6 is determined. The emissivity of the side wall ϵ_W is then determined from this starting value.

Eq. 6: $\epsilon_{Aeff}(0) = Q_E(0) / (dT \cdot 5,670367)$, $dT = T_V^4/10^8 - T_H^4/10^8$, $\epsilon_W = 1 - \epsilon_{Aeff}$ (in air)

The addition of CO2 reduces the effective emissivities of the aerosol plate $\epsilon_{Aeff}(n)$, since the CO2-radiation is now added to the radiation E_W , which is calculated from the respective heating $Q_E(n)$ (Eq. 7). Since sidewall and CO2 have the same temperature, they do not exchange energy with each other and cannot weaken each other as long as the sum $\epsilon_W + \epsilon_{CO2} < 1$. It is therefore assumed that ϵ_W remains constant during a trial. The CO2 emissivities $\epsilon_{CO2}(n)$ are calculated from the effective emissivities $\epsilon_{Aeff}(n)$ and the emissivity ϵ_W according to Eq. 7

Eq. 7: $\epsilon_{Aeff}(n) = Q_E(n) / (dT \cdot 5,670367)$; $\epsilon_{W+CO2}(n) = 1 - \epsilon_{Aeff}(n)$; $\epsilon_{CO2}(n) = \epsilon_{W+CO2}(n) - \epsilon_W$

The experimental determination of the CO₂ emissivities with the experimental apparatus has the great advantage over computational models that it includes all aspects of the complex CO₂ radiation (influence of the rotation lines, air temperatures, overlay with the cloud radiation, etc.).

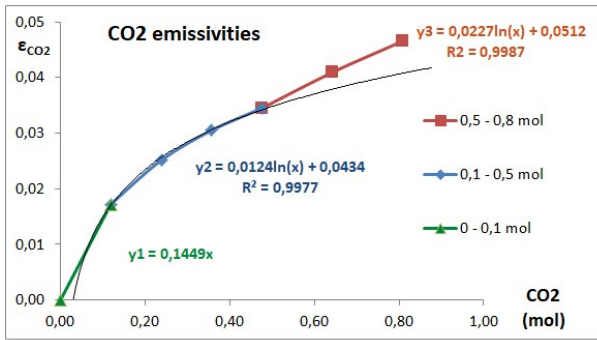


Fig. 12: Different development of CO₂ emissivities by increasing the CO₂ concentration (molar amount)

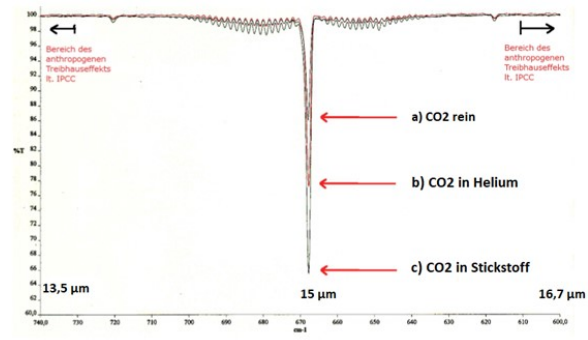


Fig. 13: Three CO₂ absorption spectra with the same CO₂ molar amount Conc.: a = 100 %, b, c = 3,5 Vol.-% in He or N₂ by H. Hug [16]

The graphical evaluation of CO₂ emission levels shows no consistent trend (Fig. 12). The course of CO₂ radiation is characterized by three different trend lines (Y1, Y2 and Y3). At first glance an unsatisfactory result, but then the diagram turns out to be a surprise and a small sensation:

Despite the very simple apparatus, the trend lines Y1 and Y2 can be interpreted as the result of vibrations (Y1) and rotations (Y2) of the CO₂ molecule!

The trend lines reflect the radiation possibilities of the CO₂ molecule. At a certain wavelength (line), CO₂ cannot produce a higher radiation density than a black emitter at the same temperature and wavelength. If the CO₂ radiation of a certain wavelength reaches the maximum value, it is called a saturation of this line. Now, the CO₂ valence vibration at 15 μm is much more intense than the outward-flattening CO₂ rotation lines (Fig. 13). After the first CO₂ addition of 0.1 mol (1 vol. %, 2500 ppm), the 15 μm line is saturated and can be provisionally calculated by a linear function Y1 (makeshift, since two data points are insufficient for a correct description). The further course up to a molar amount of 0.5 mol CO₂ follows very well a logarithmic function (equation 8.1). This course of Y2 is the actual goal of the investigation. Hereby the further progression of atmospheric CO₂ radiation can be calculated above the current 400 ppm.

Eq. 8.1: $\epsilon_{CO_2}(n) = 0,0124 \cdot \ln(n) + 0,0434$; for $c_{CO_2} < 1$ Vol.-%

Eq. 8.2: $\epsilon_{CO_2}(n) = 0,0194 \cdot \ln(n) + 0,0481$; for $c_{CO_2} > 1$ Vol.-%

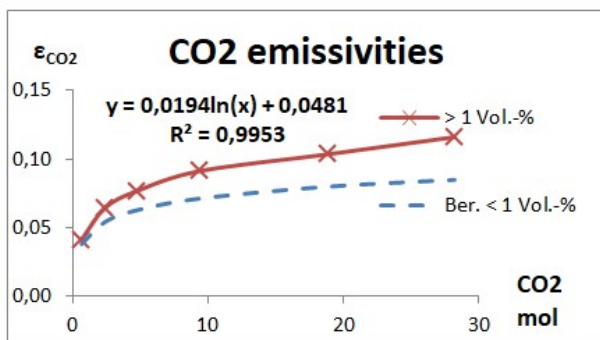


Fig. 14: CO₂ Emissivities at high concentrations > 1% and calculation according to Eq. 8.1 for < 1%

Above 1 vol. % (0.5 mol), the logarithmic course of CO₂ emissivities ends and an unexpected increase in CO₂ radiation with the trend line Y3 (red acid) occurs. A phenomenon that could be reproduced very well and it

was found at high concentrations in all investigated greenhouse gases. A control experiment above 1% up to 60 vol.-% CO₂ (30 mol) again shows a logarithmic trend, now over the entire range and with a slightly higher correlation factor (equation 8.2 and Fig. 14). The remarkable rise between Y2 and Y3 could be clarified as a concentration effect. Since this mechanism says a lot about the radiation of greenhouse gases, this chapter has its own chapter.

2.1. The CO₂ concentration effect

When determining the CO₂ absorption with an FT-IR spectrometer, Heinz Hug had observed that with the same amount of CO₂, the extinction in dilution with IR-inactive gases (helium or nitrogen) is greater than with pure CO₂ (Fig. 13) [16]. To understand the effect, one must know that CO₂ molecules only absorb electromagnetic radiation when they are in the so-called ground state. In IR irradiation, however, the CO₂ molecules are put into the excited vibration/rotation state. The energy absorption (attenuation of the IR light) would come to a halt after a short time, when all CO₂ molecules have moved into the excited state. That this is not the case is because the excited CO₂ molecules fall back to the ground state after a very short time (relaxation time) and the energy absorbed either by emission of a photon or by thermalization (energy transfer to IR-inactive gas molecules or the cuvette wall) give it up again. Ultimately, a balance of excited and unexcited molecules is created, which is influenced by the inert gases. The intensity of absorption is therefore dependent not only on the formal CO₂ concentration but also on this excitation ratio, which H. Hug has demonstrated through his concentration experiment.

However, the excited state can also be caused by collisions of the gas molecules. Even without electromagnetic irradiation, a part of the CO₂ molecules is in an excited state. The concentration effect finds its explanation in the type of molecule collisions. In high dilution by IR-inactive gases, the CO₂ molecules collide exclusively with the inert gases. The kinetic energy is absorbed either by the CO₂ or by the inert gas. With increasing CO₂ concentration, however, the probability that two CO₂ molecules collide increases, which increases their chance of excitation. In other words, with increasing CO₂ concentration, the number of excited CO₂ molecules increases: A) by the increase in concentration (number of CO₂ molecules) and B) by the higher stimulation chance. The excited CO₂ molecules can fall back into the ground state through a spontaneous or induced emission and release the energy in the form of photons, which explains the higher CO₂ emission with the trend line Y3 (Fig. 12). The quantitative effect of the concentration effect is shown in Fig. 14 as the distance between blue (measured) curve for high CO₂ concentrations and red dashed line curve (calculated) for small CO₂ concentrations.

In summary, CO₂ concentrations > 1% by volume increase the number of excited CO₂ molecules disproportionately, which in the absorption spectra leads to a weakening of the absorption (Fig. 13), but in the CO₂-radiation experiments (Fig. 12) leads to an increase in the emission.

What does this knowledge mean? The effect cannot be applied to the atmospheric CO₂, since the concentration of around 0.04% by volume is far below the critical threshold of 1% by volume. In the following, therefore, the CO₂ emissivity is calculated only with formula 8.1. In the case of water vapor, which can reach up to 4% by volume in the near-Earth atmosphere, a concentration effect could be of importance.

3. The CO₂ radiation formula

The CO₂ emissivities were determined from the experimentally determined CO₂ emissions, including the temperatures for the foreground and background. It therefore makes sense to simply reverse this procedure

and to calculate the effective CO₂ radiation from the molar CO₂ emissivities $\epsilon_{CO_2}(n)$ with the temperatures for the foreground and background. The CO₂ radiation E_{CO_2} is the actual, effective CO₂ contribution to the irradiation of the earth of 1 m², the so-called radiation amplification of an already existing background radiation. The effective CO₂ radiation depends on the CO₂ temperature, CO₂ molar amount and the temperature of the clouds/aerosols. If the CO₂ radiation is calculated without background ($T_H = 0$), E_{CO_2} means the theoretical maximum possible CO₂ radiation.

Eq. 9
$$E_{CO_2}(n) = \epsilon_{CO_2}(n) \cdot \sigma \cdot (T_V^4/10^8 - T_H^4/10^8)$$

This empirically derived equation is almost identical to Stefan's Eq. 2 for the heat loss of the hot thermometer, except that now the CO₂ emissivities $\epsilon_{CO_2}(n)$ have been added. Eq. 9/8.1 and 9/8.2 now allow the CO₂ emissions of the laboratory experiments to be calculated. Calculated and measured values show good agreement (Fig. 15 and 16).

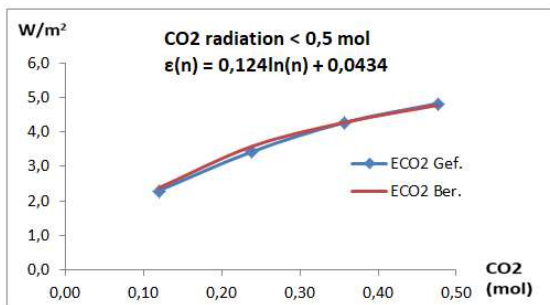


Fig. 15: Calculated and found CO₂ radiation values acc. to Eq. 9/8.1

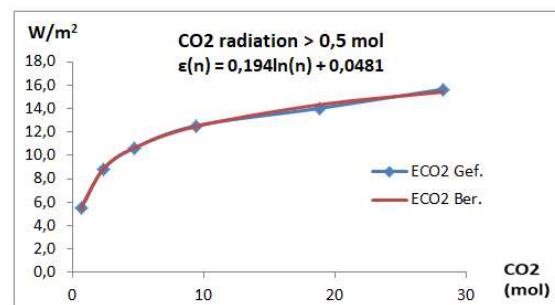


Fig. 16: Calculated and found CO₂ radiation values acc. to Eq. 9/8.2

The relativity of CO₂ radiation, the radiation amplification of an already existing background radiation, is described in Eq. 9 expressed by the temperature difference $T_V(\text{CO}_2)$ and $T_H(\text{clouds/aerosols})$. Here, T_V is the air temperature of the near-Earth air layer and T_H is the radiation temperature of the clouds/aerosols (in Kelvin), which can be measured with a pyrgeometer in the atmospheric window at around 10 μm. In low clouds or in fog, when $T_H = T_V$, the expression $(T_V^4/10^8 - T_H^4/10^8)$ becomes zero and CO₂, no matter in which concentration, loses its greenhouse effect.

From 2016 to 2017 measurements of background and air temperatures in Berlin showed a temperature difference of around 40 °C in clear skies and 8 °C in covered skies. [12]. Of course, these measurements are not representative of the Earth, but they give an idea of what reduction of the theoretical CO₂ radiation is to be expected when background radiation is taken into account (Tab. 1).

Tab. 1: The effective CO₂ radiation in percent to the theoretical radiation (air = 15 °C)

Temperature difference of foreground and background					
0 °C	8 °C	10 °C	20 °C	30 °C	40 °C
Effective CO ₂ radiation					
0%	11%	13%	25%	36%	45%

4. The atmospheric CO₂ radiation

Climatologists calculate atmospheric CO₂ radiation using complex computational models, initially evaluating many hundreds of lines of a high-resolution CO₂ spectrum (Fig. 17). Subsequently, with the temperatures of the troposphere, tropopause and stratosphere, radiation equilibria of these weighted lines are calculated.

This is a huge effort that ordinary people can neither understand nor comprehend. Perhaps for this reason, Ramaswamy et al. [2] set up with the obtained values for the CO2 back radiation a simple relationship between CO2 concentration and radiation, the so-called radiation force dF . The concept of radiation forcing is based on the thesis that the world is in a sensitive, thermal equilibrium, which can be brought out of balance even by the smallest changes, by a force (dF). An easily measurable change is the CO2 concentration, which has increased steadily since 1750 (the beginning of industrialization) from 278 to today's 400 ppm. With Eq. 10, according to Ramaswamy, the additional CO2 radiation of this concentration increase is calculated.

Eq. 10: $dF = 5.35 \cdot \ln(c/c_0)$ in W/m^2 , $c_0 = 278$ ppm

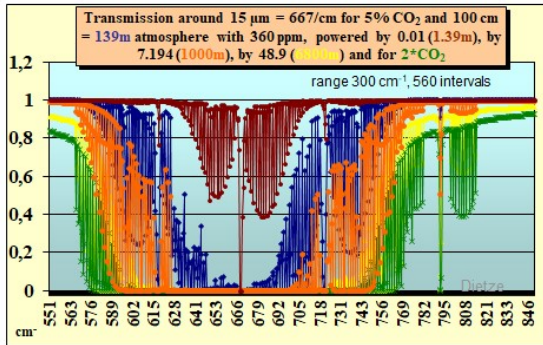


Fig. 17: High-resolution CO2 spectra acc. to Peter Dietze [7]

CO2		dF
c	$c_0 = 278$	
ppm	$\ln(c/c_0)$	W/m^2
278	0,00	0,00
300	0,08	0,41
325	0,16	0,84
350	0,23	1,23
375	0,30	1,60
400	0,36	1,95

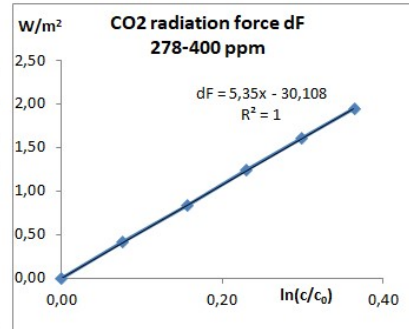


Fig. 18: Increase of the CO2 radiation force of $1.95 W/m^2$ since 1750 acc. to IPCC-Eq. 10

However, the calculation obscures the absolute CO2 radiation and the actual CO2 share of the global back radiation, but this can be derived from Eq. 10 as follows. For this purpose, the radiation force dF was calculated for the CO2 concentrations of 278 to 400 ppm according to Eq. 10 and plotted as $\ln(c/278)$ in an Excel chart (Fig. 18). With the help of the trend line, a value of minus 30.108 is obtained for $x = 0$ (278 ppm CO2). This can be used to determine the CO2 radiation for the year 1750 at $30.11 W/m^2$. Adding this value to Eq. 10 gives Eq. 11, which can now be used to calculate the absolute CO2 radiation. Accordingly, 400 ppm of CO2 generates a back radiation of $32.1 W/m^2$ ($30.11 + 1.95$) or 9.6% of the global back radiation of $333 W/m^2$ (Fig. 1, 19).

Eq. 11: $E_{CO2} = 5.35 \cdot \ln(c/278) + 30.11 W/m^2$

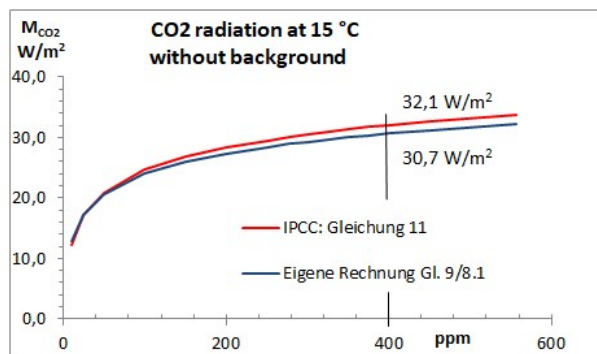


Fig. 19: Theoretical CO2 radiation acc. to IPCC-Eq. 11 and acc. Eq. 9/8.1 without background radiation

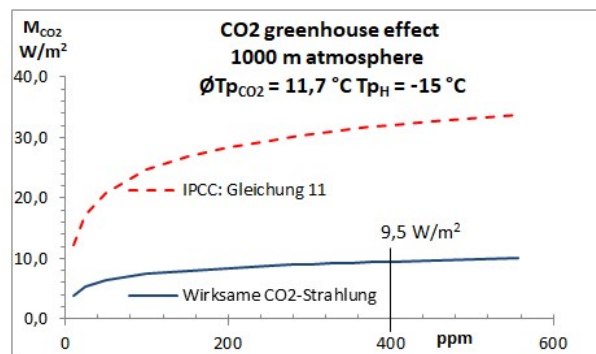


Fig. 20: Effective CO2 radiation acc. to Eq. 9/8.1 under a cloud/aerosol layer $T_{pH} = -15$ °C

Kiehl and Trenberth indicate a share of back radiation (excluding clouds) of 9 to 26% for CO2 [17]. The smaller number stands for the mixture of CO2 with other greenhouse gases and the larger number for pure

CO₂. The value of 9% CO₂ coincides with the above calculation according to IPCC equation 11, but it also leads to a conflict, since with this small CO₂ value the back radiation of the 333 W/m² cannot be explained. For water vapor, the same authors give a share of 36 - 70%. If one calculates with the smaller numbers (9 and 36% for gas mixtures), water vapor and CO₂ only have a total proportion of 45% of the atmospheric back radiation. Accordingly, 55% or 183 W/m² does not come from these greenhouse gases, but from the clouds/aerosols (and some trace gases). This is a blatant contradiction to the alleged cloud greenhouse effect of only 30 W/m² [3].

Now CO₂ radiation can also be calculated with the experimentally found Eq. 9/8.1. In the case of a calculation under normal conditions but without a background (see below), a radiation curve (blue) is obtained which agrees remarkably well with the IPCC curve (red) (Fig. 19, Tab. 2). The good agreement is further confirmation that 400 ppm CO₂ at 15 ° C will actually only produce a radiation of 31-32 W/m² if the clouds/aerosol radiation is excluded.

However, taking into account the radiation of the clouds/aerosols, there is a further reduction of the effective CO₂ radiation from 32 to now 9.5 W/m² (3% of global back radiation). This value is obtained if in Eq. 9/8.1 for the background a realistic temperature of -15 ° C (instead of -273 ° C, without background) is used. This reduction in CO₂ radiation is due to the fact that CO₂ uses the same wavelengths that also emit clouds/aerosols, causing premature saturation. The common radiation is governed by the principle of foreground and background radiation. According to this, even without greenhouse gases, the Earth already receives a back radiation of around 275 W/m² due to the background radiation of the clouds/aerosols [4]. The presence of CO₂ (32 W/m²) and water vapor (0.36 · 333 = 120 W/m²) as foreground emitter leads to an overlay with the already existing background radiation and results an amplification by CO₂ and H₂O (orange, blue), whereby the back radiation only increases by 58 W/m² to 333 W/m² (Fig. 21). The energy scheme refutes the thesis of a fragile balance. Every change of an IR-emitter causes a counter reaction of the other radiation sources and indicates a robust radiation system.

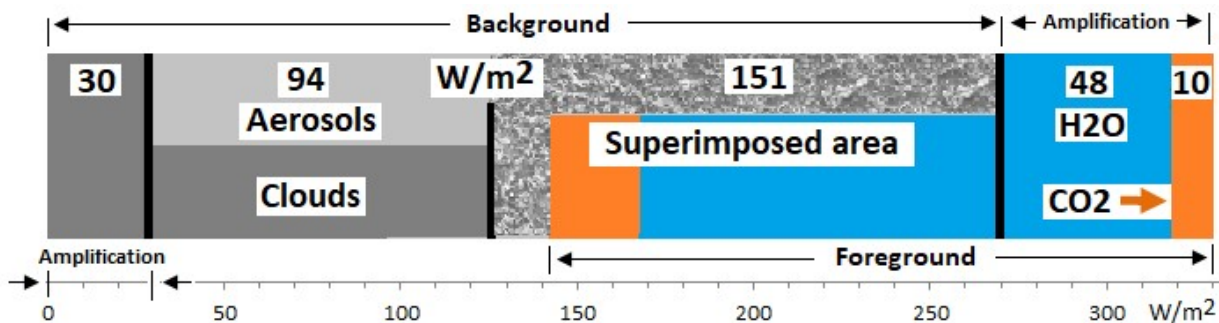


Fig. 21: Energy scheme of the atmospheric back radiation of 333 W/m² acc. to the principle of the fore- and background radiation

Thus, the seemingly low cloud greenhouse effect is only an increase in aerosol radiation of 30 W/m², while most of the cloud radiation is hidden in the superimposed area. With this consideration, the cloud/IR gas paradox can be solved.

The clouds/greenhouse gas paradox [11]: In measurements of atmospheric back radiation, contrasting results were found:

A) *At different humidity's: clouds dominant (water vapor had low effect) [18].*

B) *In clear and cloudy skies: water vapor dominant (cloud had low effect) [5].*

The contradiction is resolved when it is considered that varying an atmospheric radiation source (water vapor, degree of cloudiness) not their radiation, but only their radiation amplification is measured.

The following calculations on atmospheric CO2 radiation according to Eq. 9/8.1 are rollover calculations used to transfer laboratory tests to the atmosphere. First, you need the range of the CO2 radiation that is the layer thickness, which just contributes to a radiation amplification of the Earth's surface. Step by step, air layers of 25 to 2,000 m thickness are analyzed. The pressure, temperature and CO2 molar mass of these layers are calculated from the barometric formula, a temperature gradient of 0.65 K/100 m and the ideal gas equation. Temperature and pressure are considered as the average of a layer. The radiation temperature of the background was arbitrarily assumed to be -15 °C, for lack of known values. According to Eq. 9/8.1 the CO2 radiation of each layer (related to height = 0) is calculated. Air layers above 1,000 m are therefore no longer contributing to the increase in CO2 radiation, which is mainly caused by the decrease in the temperature difference $dT = (T_V^4/10^8 - T_H^4/10^8)$. Also noteworthy is the 50% value, which is around 25 m and emphasizes the short range of CO2 radiation (Fig. 22).

T_{pH} °C	T_p . Luft	CO2	n = pV/RT			CO2- Strahlung
-15,0	0,65 °/100 m	400 ppm	$p=1013,25(1-(0,0065 \cdot H/2)/288,15)^{5,255}$			
Höhe m	Ø Druck hPa	Ø T_{pLuft} °C	n mol	ϵ_{CO_2} A)	dT K	E_{CO_2} W/m ²
$R = 8,31 \text{ J}/(\text{mol} \cdot \text{K}); V = H \cdot A \text{ (m}^3); A = 1 \text{ m}^2$						Gl. 9/8.1
0	1013	15,00	0,0	0,000	24,53	0
25	1012	14,92	0,422	0,033	24,45	4,54
50	1010	14,84	0,844	0,041	24,37	5,71
100	1007	14,68	1,684	0,050	24,22	6,85
200	1001	14,35	3,351	0,058	23,91	7,92
300	995	14,03	5,002	0,063	23,60	8,48
400	989	13,70	6,638	0,067	23,29	8,83
500	984	13,38	8,257	0,070	22,99	9,07
800	966	12,40	13,022	0,075	22,07	9,42
1000	955	11,75	16,120	0,078	21,47	9,48
1200	943	11,10	19,157	0,080	20,87	9,47
1400	932	10,45	22,133	0,082	20,28	9,41
1600	921	9,80	25,049	0,083	19,69	9,30
2000	899	8,50	30,704	0,086	18,52	9,02

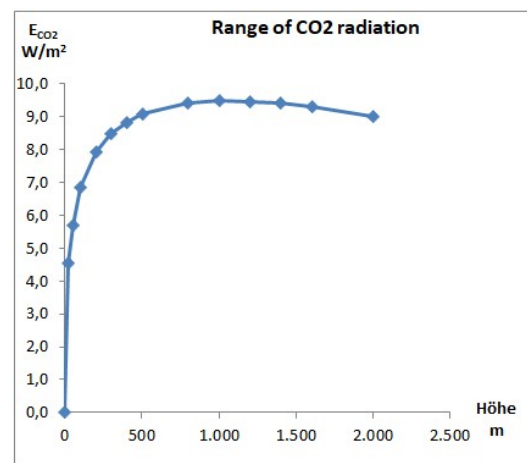


Fig. 22: Determination of the maximum range of CO2 radiation acc. to Eq. 9/8.1

With the determined range of 1,000 m and the associated pressure and temperature values, the concentration-dependent CO2 radiation without background (Fig. 18, 23) and the CO2 radiation amplification (Fig. 1 and 19) were calculated.

CO2-Strahlung: 1000 m Atmosphäre, Wolken/Aerosole = -273,15 °C						
ppm	Ø Druck	Ø T_{pLuft} °C	n	A) ϵ_{CO_2}	dT	E_{CO_2}
10	955	11,75	0,4	0,032	65,88	12,01
25	955	11,75	1,0	0,043	65,88	16,25
50	955	11,75	2,0	0,052	65,88	19,46
100	955	11,75	4,0	0,061	65,88	22,67
150	955	11,75	6,0	0,066	65,88	24,55
200	955	11,75	8,1	0,069	65,88	25,88
250	955	11,75	10,1	0,072	65,88	26,92
278	955	11,75	11,2	0,073	65,88	27,41
300	955	11,75	12,1	0,074	65,88	27,76
325	955	11,75	13,1	0,075	65,88	28,13
350	955	11,75	14,1	0,076	65,88	28,47
375	955	11,75	15,1	0,077	65,88	28,79
400	955	11,75	16,1	0,078	65,88	29,09
450	955	11,75	18,1	0,079	65,88	29,64
556	955	11,75	22,4	0,082	65,88	30,62

CO2-Strahlung: 1000 m Atmosphäre, Wolken/Aerosole = -15 °C						
ppm	Ø Druck	Ø T_{pLuft} °C	n	B) ϵ_{CO_2}	dT	E_{CO_2}
10	955	11,75	0,4	0,032	21,47	3,91
25	955	11,75	1,0	0,043	21,47	5,30
50	955	11,75	2,0	0,052	21,47	6,34
100	955	11,75	4,0	0,061	21,47	7,39
150	955	11,75	6,0	0,066	21,47	8,00
200	955	11,75	8,1	0,069	21,47	8,44
250	955	11,75	10,1	0,072	21,47	8,77
278	955	11,75	11,2	0,073	21,47	8,93
300	955	11,75	12,1	0,074	21,47	9,05
325	955	11,75	13,1	0,075	21,47	9,17
350	955	11,75	14,1	0,076	21,47	9,28
375	955	11,75	15,1	0,077	21,47	9,38
400	955	11,75	16,1	0,078	21,47	9,48
450	955	11,75	18,1	0,079	21,47	9,66
556	955	11,75	22,4	0,082	21,47	9,98

Fig. 23: CO2 radiation: Air layer = 1000 m according to Eq. 9/8.1: Left without background radiation (-273 °C), right: background = -15 °C

Tab 2: CO2 radiation without background under normal conditions, air layer = 1,000 m, acc. Eq. 9/8.1 and IPCC Eq. 11

CO2: ppm	25	50	100	150	200	250	278	300	325	350	375	400	450	556
CO2: n	1,1	2,1	4,2	6,3	8,5	10,6	11,8	12,7	13,7	14,8	15,9	16,9	19,0	23,5
ϵ_{CO_2}	0,044	0,053	0,061	0,066	0,070	0,073	0,074	0,075	0,076	0,077	0,078	0,078	0,080	0,083
E_{CO_2}	17,2	20,6	24,0	25,9	27,3	28,4	28,9	29,3	29,7	30,0	30,4	30,7	31,2	32,3
IPCC: Gl. 11	17,2	20,9	24,6	26,8	28,3	29,5	30,1	30,5	30,9	31,3	31,7	32,1	32,7	33,8

5. Annex - Experimental Data

Determining CO2 emissions is more difficult than simply demonstrating the greenhouse effect (Fig. 8). After each addition of CO2, the voltage for the heater Q_E is reduced until the start temperature of the earth plate of 16.09 ° C is just reached again. Since the system of heating and temperature measurement has certain inertia, the average of two measurements is formed at intervals of 0.01 to 0.02 volts, both of which give a temperature of 16.09 ° C. The experiments were repeated 3 to 5 times and rated as an average.

The earth plate has a diameter of 16.7 cm and an area $A_E = 219.04 \text{ cm}^2$. The heating Q_E of the earth plate is converted by multiplication with 45.654 to a square meter $A_E = 1 \text{ m}^2$. The distance between earth and aerosol plate is 1.11 m. The molar amount thus refers to a fictitious volume of 1.11 m^3 .

5.1. 5.1. CO2 emissivities up to 0.8 mol (1.7 vol. %).

5 Versuche (\emptyset) Nr. 169, 170, 194, 195, 196; $\epsilon_W = 0,268$									
T_{PE} °C	T_{PA} °C	$\emptyset T_{p_{Luft}}$ °C	Druck hPa	Q_E W/m ²	CO2 Vol.-%	CO2 mol	ϵ_A	ϵ_{W+CO_2}	ϵ_{CO_2}
16,09	-14,52	15,45	1029,8	102,21	0,00	0,00	0,732	0,268	0,000
16,09	-14,60	15,42	1030,0	99,91	0,25	0,12	0,715	0,285	0,017
16,09	-14,60	15,42	1030,0	98,78	0,50	0,24	0,707	0,293	0,025
16,09	-14,56	15,42	1029,3	97,94	0,75	0,36	0,701	0,299	0,031
16,09	-14,57	15,41	1028,4	97,39	1,00	0,48	0,697	0,303	0,034
16,09	-14,54	15,43	1028,3	96,49	1,35	0,64	0,691	0,309	0,041
16,09	-14,59	15,45	1028,0	95,90	1,70	0,81	0,685	0,315	0,047

5.2. CO2 emissivities up to 28.2 mol (60 vol.-%)

3 Versuche (\emptyset) Nr. 134, 144, 152; $\epsilon_W = 0,242$									
T_{PE} °C	T_{PA} °C	$\emptyset T_{p_{Luft}}$ °C	Druck hPa	Q_E W/m ²	CO2 Vol.-%	CO2 mol	ϵ_A	ϵ_{W+CO_2}	ϵ_{CO_2}
16,09	-14,20	15,14	1017,2	103,57	0,00	0,00	0,758	0,242	0,000
16,09	-14,29	15,09	1017,3	98,00	1,38	0,65	0,717	0,283	0,041
16,09	-14,24	15,10	1016,7	94,74	5,00	2,35	0,694	0,306	0,064
16,09	-14,21	15,08	1016,2	92,94	10,00	4,71	0,682	0,318	0,076
16,09	-14,22	15,10	1016,0	91,03	20,00	9,41	0,667	0,333	0,091
16,09	-14,29	15,10	1015,7	89,54	40,00	18,82	0,655	0,345	0,103
16,09	-14,27	15,13	1016,0	87,90	60,00	28,23	0,642	0,358	0,116

5.3. 5.3. Effective radiation E_A in air

Versuch Nr. 205								
T_{pE} °C	T_{p1} °C	T_{p2} °C	T_{p3} °C	T_{p4} °C	T_{pA} °C	T_A K	Q_E W/m ²	E_A W/m ²
16,1	16,1	16,1	16,1	16,2	15,7	69,7	0,0	291,5
16,1	15,9	15,8	15,9	15,8	7,6	62,1	29,7	259,8
16,1	15,7	15,7	15,7	15,6	-0,4	55,4	56,9	231,8
16,1	15,6	15,7	15,6	15,5	-6,0	51,0	74,9	213,3
16,1	15,5	15,6	15,5	15,4	-10,4	47,6	90,1	199,4
16,1	15,5	15,6	15,5	15,2	-14,5	44,8	103,4	187,5
16,1	15,4	15,5	15,4	15,3	-17,6	42,6	113,3	178,4

Bibliography

- [1] K. E. Trenberth et al., „EARTH’S GLOBAL ENERGY BUDGET,“ 19 Juli 2008. [Online]. Available: https://www.klimamanifest-von-heiligenroth.de/wp/wp-content/uploads/2016/09/Trenberth_Jones_Treibhauseffekt_TFK_bams_2009_15Grad_390Watt_SBG_gelb_Mark.pdf
- [2] V. Ramaswamy et al., „Radiative Forcing of Climate Change,“ März 2018. [Online]. Available: <https://www.ipcc.ch/site/assets/uploads/2018/03/TAR-06.pdf>.
- [3] „Wolken im Klimasystem,“ 23 Oktober 2017. [Online]. Available: http://wiki.bildungsserver.de/klimawandel/index.php/Wolken_im_Klimasystem.
- [4] M. Schnell, „2. Mitteilung: Die Hintergrundstrahlung der Wolken und Aerosole,“ 2018 Juni 2018. [Online]. Available: <https://www.eike-klima-energie.eu/2018/06/03/experimentelle-verifikation-des-treibhauseffektes/>.
- [5] „Atmosphärische Gegenstrahlung,“ 24 Mai 2009. [Online]. Available: https://de.wikipedia.org/wiki/Atmosph%C3%A4rische_Gegenstrahlung.
- [6] E. Roth, „Welchen Einfluss hat CO2 auf das Klima?,“ 02 Juli 2013. [Online]. Available: <http://www.energie-fakten.de/pdf/2013-07-roth.pdf>.
- [7] P. Dietze, „Berechnung der CO2-Klimasensitivität,“ 19 Oktober 2016. [Online]. Available: https://www.eike-klima-energie.eu/wp-content/uploads/2016/11/Dietze_Klimasensitivitaet_ECS-4.pdf.
- [8] J. Stefan, „Über die Beziehung zwischen der Wärmestrahlung und der Temperatur.,“ SB der Ak. d. Wiss. Wien, Math. Physikal. Kl. 79, 1879, S. 391-428, Wien, 1879.
- [9] P. Dulong, Annales de chim. de phys, Bde. %1 von %2VII. Seite 225 – 264 und 337 - 367,, 1817.
- [10] „Stefan-Boltzmann-Gesetz,“ 26 September 2018. [Online]. Available: <https://de.wikipedia.org/wiki/Stefan-Boltzmann-Gesetz>.
- [11] M. Schnell, „Experimentelle Verifizierung des Treibhauseffektes,“ 12. Internationale Klima- und Energiekonferenz (IKEK-12), München, 2018.

- [12] M. Schnell, „3. Mitteilung Labor-Experimente zur Demonstration des CO₂-Treibhauseffektes,“ 17 Juli 2018. [Online]. Available: <https://www.eike-klima-energie.eu/2018/07/17/experimentelle-verifikation-des-treibhauseffektes-2/>.
- [13] N. S. Nahle, „Repeatability of Prof. Robert Wood's 1909 Experiment on the Theory of the Greenhouse,“ 05 Juli 2011. [Online]. Available: http://www.biocab.org/experiment_on_greenhouses__effect.pdf.
- [14] A. Watts, „Replicating Al Gore's Climate 101 video experiment shows that his "high school physics" could never work as advertised,“ [Online]. Available: <https://wattsupwiththat.com/2011/10/18/replicating-al-gores-climate-101-video-experiment-shows-that-his-high-school-physics-could-never-work-as-advertised/?cn-reloaded=1>.
- [15] S. Sirtl, „Absorption thermischer Strahlung durch atmosphärische Gase. Experimente für den Physikunterricht,“ 12 November 2010. [Online]. Available: <https://docplayer.org/18989667-Absorption-thermischer-strahlung-durch-atmosphaerische-gase.html>.
- [16] H. Hug, „Der anthropogene Treibhauseffekt – eine spektroskopische Geringfügigkeit,“ 20 August 2012. [Online]. Available: <https://www.eike-klima-energie.eu/2012/08/20/der-anthropogene-treibhauseffekt-eine-spektroskopische-geringfuegigkeit/>.
- [17] „Treibhauseffekt,“ 16 Januar 2019. [Online]. Available: Literatur\Treibhauseffekt Wikipedia.pdf.
- [18] F. Albrecht, Untersuchungen über den Wärmehaushalt der Erdoberfläche in verschiedenen Klimagebieten, Bd. VIII, Berlin: Julius Springer, 1940.